Pure appl. geophys. 163 (2006) 1073–1089
0033–4553/06/061073–17
DOI 10.1007/s00024-006-0066-6

Pure and Applied Geophysics

Fracture Toughness Evaluation Based on Tension-softening Model and its Application to Hydraulic Fracturing

KAZUSHI SATO,[1] and TOSHIYUKI HASHIDA[2]

Abstract—This paper discusses the applicability of the tension-softening model in the determination of the fracture toughness of rocks, where the fracture toughness evaluated based on the tension-softening model is compared with the crack growth resistance deduced from laboratory-scale hydraulic fracturing tests. It is generally accepted that the fracture process is dominated by the growth of a fracture process zone for most types of rocks. In this study, the *J*-integral based technique is employed to determine the fracture toughness of Iidate granite on the basis of the tension-softening model, where compact tension specimens of different dimensions were tested in order to examine the specimen size effect on the measured fracture toughness. It was shown that the tension-softening relation deduced from the *J*-integral based technique allowed us to determine the specimen size independent fracture toughness K_c of Iidate granite.Laboratory-scale hydraulic fracturing tests were performed on cubic specimens (up to a 10 m sized specimen), where cyclic pressurization was conducted using a rubber-made straddle packer to observe the extent of the hydraulically induced crack. The experimental results of pressure and crack length were then used to construct the crack growth resistance curve based on the stress intensity factor *K*. The crack growth resistance obtained from the hydraulic fracturing tests was observed to initially increase and then level off, giving a constant *K* value for a long crack extension stage. The plateau *K* value in the crack growth resistance curve was found to be in reasonable agreement with the fracture toughness K_c deduced from the tension-softening relation. It was demonstrated that the tension-softening model provides a useful tool to determine the appropriate fracture toughness of rocks, which may be applicable for the analysis of the process of large-scale crack extension in rock masses.

Key words: Rock, fracture toughness, tension-softening model, hydraulic fracturing, *J*-based technique.

1. Introduction

The hydraulic fracturing is one of the most promising methods for enhancing the recovery of geothermal energy from a deep rock mass. Because the size of the subsurface cracks induced hydraulically is important to the heat exchange process, a fracture mechanics approach is expected to provide a useful tool in the development

[1]Miyagi National College of Technology, 48 Aza Nodayama, Shiote, Medeshima, Natori, 981–1239, Japan. E-mail: kazushi@miyagi-ct.ac.jp
[2]Fracture and Reliability Research Institute, Tohoku University, 01 Aoba, Aramaki, Aoba-ku, Sendai, 980–8579, Japan

of the artificial geothermal energy extraction system. The prediction of the crack size calls for the determination of appropriate fracture toughness of rocks, initially.

It is well known that the fracture process of rocks is dominated by the growth of a fracture process zone (LABUTZ *et al.*, 1987). The crack growth resistance of rocks increases with the growth of the fracture process zone, as is often observed in rising crack growth resistance curves for many types of rocks. After the fracture process zone is fully formed and the steady-state of crack growth is achieved, then the crack growth resistance curve levels off and saturates, giving the constant value of crack growth resistance. In order to analyze the growth of hydraulically induced cracks on a field scale, the saturated and constant crack growth resistance must be determined for the rock of concern. It has been shown that apparent fracture toughness values determined on the basis of linear elastic fracture mechanics (LEFM) increases with respect to specimen size, and that a valid K_{Ic} test for rocks generally requires an impracticably large specimen size (SCHMIDT and LUTZ, 1979: INGRAFFEA, 1987: HASHIDA and TAKAHASHI, 1993). The difficulty can be generally attributed to the non-negligible size of the fracture process zone, which is often comparable with the specimen dimension used for the laboratory-scale fracture toughness tests. Therefore, the above-mentioned results indicate that it may be difficult to employ LEFM-based testing methods to evaluate the appropriate crack growth resistance and then the fracture toughness for the analysis of the field scale crack extension. Hence, a suitable model for characterizing the formation of the fracture process zone is necessary in order to evaluate the fracture toughness on the basis of laboratory experiments.

The use of a Barenblatt-type cohesive crack model has been proposed by HILLERBORG (1983) for concrete. This cohesive crack model is often referred to as the tension-softening model for the crack opening mode. As illustrated in Figure 1, the tension-softening model represents the fracture process zone as an extension of the crack subjected to a closing stress σ which depends on the crack opening displacement δ of the fictitiously extended crack. The relation between the cohesive stress σ and the crack opening displacement δ is called the tension-softening curve. By definition, the tension-softening curve can be obtained from a direct tension test. Therefore, the peak of the cohesive stress corresponds to the uniaxial tensile strength. Furthermore, the area under the tension-softening curve provides the critical J-integral value which corresponds to the crack growth resistance for the steady-state of crack growth after the fracture process zone is fully formed. Consequently, the fracture toughness for the analysis of the hydraulically induced crack may be evaluated by the measurement of the tension-softening curve in laboratory tests.

In this paper, we investigate the usefulness of the fracture toughness based on the tension softening model for the prediction of the growth of hydraulically induced cracks. By employing the J-integral based testing method, fracture tests were conducted to determine the tension softening relation of a granite using fracture toughness specimens of various sizes. The appropriate fracture toughness of the

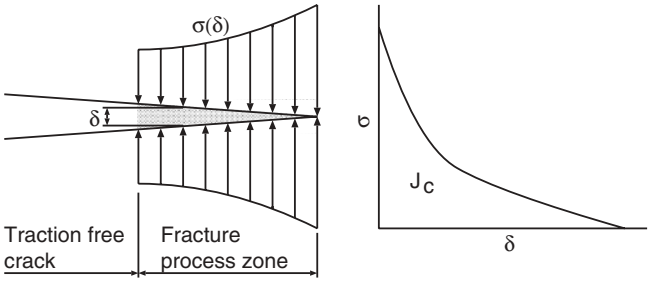

Figure 1
Schematic drawing of the tension–softening model. Fracture process zone is represented by a fictitious crack with cohesive stress. The relation between the cohesive stress and the crack opening displacement of the fictitious crack is the tension-softening curve.

granite was determined by examining the effect of the specimen size on the measured tension softening relation. Laboratory-scale hydraulic fracturing tests were performed to evaluate the crack growth resistance curve of the granite. The crack growth resistance curve was evaluated using the stress intensity factor. The crack growth resistance curve obtained from the hydraulic fracturing tests was compared with the fracture toughness value in order to examine the validity of the tension softening model for rocks.

2. Fracture Toughness Test

This section presents the results of fracture toughness tests of a granite based on the tension-softening model. The *J*-based technique is used to measure the tension-softening curve. The fracture toughness deduced from the tension-softening curve is compared with the fracture mechanics parameters estimated from the fracture energy method and the crack growth resistance approach.

In principle, the tension-softening curve can be evaluated by conducting direct tensile tests. However, it is generally very difficult to perform a stable direct tensile test and to obtain the complete stress-displacement curve. Li *et al.,* (1987) have introduced a *J*-based technique for determining the tension-softening curve for concrete. In this technique, a set of fracture toughness tests are conducted instead of the direct tension test, and the load vs. load-line displacement relation registered is used to produce the tension-softening curve. The technique allows us to perform a stable fracture test using a conventional testing machine. In the following, a brief description of the *J*-based technique is presented.

The *J*-based technique is based on the nonlinear fracture mechanics parameter, *J*-integral. Taking advantage of a cohesive crack model, the area under the tension-softening curve is related to the *J*-integral

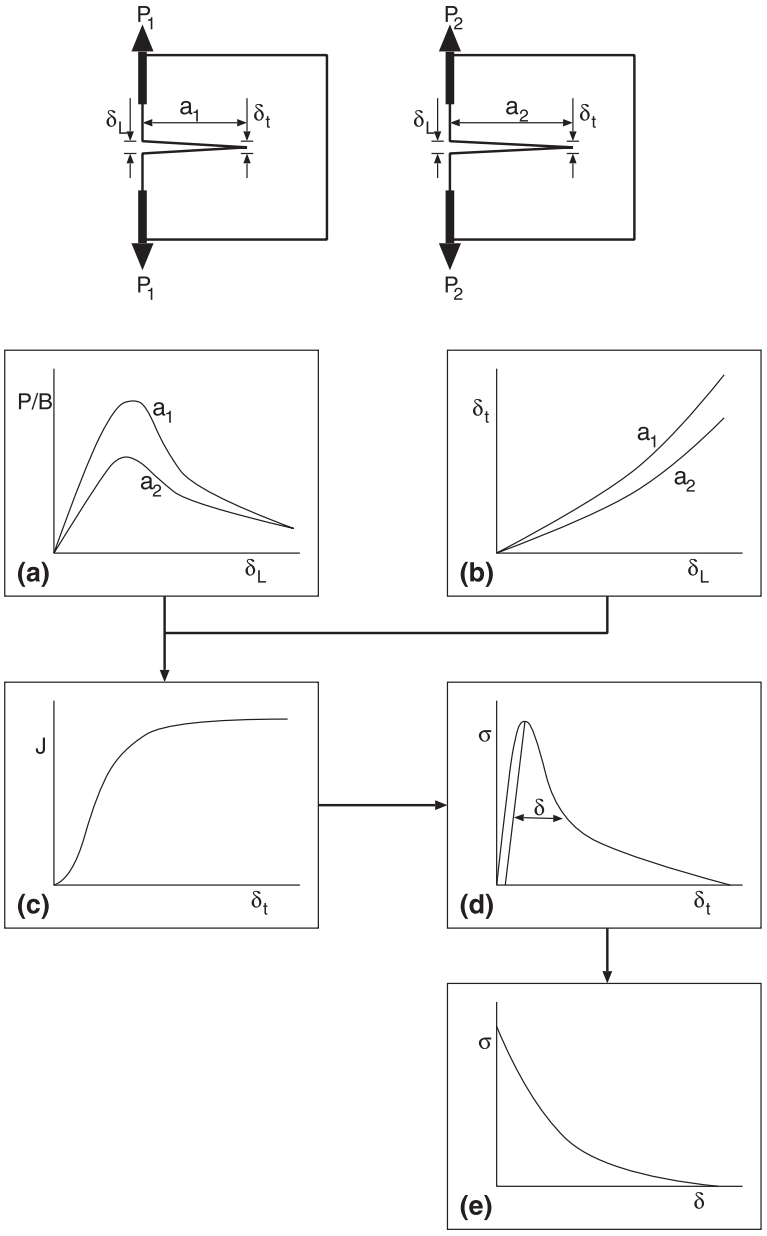

Figure 2
Flow chart of testing procedure by the J-based technique.

$$J = \int_0^{\delta_t} \sigma \, d\delta, \tag{1}$$

where δ_t is the crack opening displacement at the initial crack tip. Differentiating Equation (1) with respect to δ_t, the cohesive stress σ may be determined from

$$\sigma = \frac{\partial J}{\partial \delta_t}. \tag{2}$$

Thus, if the relation between J and δ_t can be obtained experimentally, the tension-softening curve can be derived from Equation (2).

Figure 2 illustrates the flow of the testing procedure of the J-based technique. The J-integral value can be evaluated experimentally by conducting tests on two specimens with slightly different crack lengths. During the tests, load P, load line displacement δ_L and crack tip opening displacement δ_t are measured simultaneously. The value of the J-integral for a given value of δ_L is calculated using the following equation

$$J(\delta_L) = \frac{1}{a_2 - a_1} \int_0^{\delta_L} \left(\frac{P_1}{B_1} - \frac{P_2}{B_2} \right) d\delta_L, \tag{3}$$

where B is the specimen thickness. The subscripts, 1 and 2, refer to the different crack lengths, a_1 and a_2, respectively. Based on a set of P/B-δ_L and δ_t-δ_L relations for each specimen with different crack lengths, the relation between J and δ_t is obtained as in Figure 2(c). In this procedure, the average of the crack tip opening displacement for each specimen is used as δ_t. Figure 2(d) indicates the σ-δ_t relation deduced from the slope of the J-δ_t data. The initial rising portion of the σ-δ_t curve is due to an elastic deformation between the measuring points of δ_t, and therefore should not be regarded as part of the tension-softening curve. Assuming the unloading path from the peak of the curve which is parallel to the initial slope of the curve, and subtracting the elastic deformation, the true crack opening displacement δ is extracted from the measured δ_t as shown in Figure 2(d). Figure 2(e) shows the corrected tension-softening curve.

The above-mentioned procedure was employed to measure the tension-softening curve using compact tension (CT) specimens of various sizes and to determine the valid fracture toughness based on the tension-softening model. The rock tested was granite from a quarry in Iidate, Fukushima prefecture, Japan. Iidate granite is a light gray biotite granite, containing a rift plane typical of granites. In this study, four blocks of Iidate granite were used to conduct fracture toughness tests and hydraulic fracturing tests. As shown in Table 1, the fracture property of the individual blocks was found to be slightly different, depending on the sampling location of the quarry. Hereafter, in order to distinguish the sampling locations, the four rock blocks used are labeled as A, D, F and H, respectively. The geometry of the CT specimen used is shown in Figure 3. The specimen dimensions are given in Table 2. The CT specimens

Table 1

Elastic and fracture properties measured for four blocks of Iidate granite.

Rock	E' (GPa)	J_c (N/m)	$K_c(=\sqrt{E'J_c})$ (MPa$\sqrt{m}$)	σ_f (MPa)	σ_{uts} (MPa)
A	41.9	163	2.71	5.78	5.38
D	29.6	386	3.38	5.61	4.83
F	59.5	166	3.14	7.28	—
H	36.3	112	2.00	3.28	—

of several different sizes were tested for Rock A to examine the specimen size effect on the measured tension-softening curve (HASHIDA, 1989). Side grooves, width 4.3 mm and depth 7.0 mm, were machined into the specimen to enforce the crack growth to remain in the median plane. An artificial notch of width of 0.15 mm was introduced in each specimen. Hashida and Takahashi (1993) verified that the notch width of 0.15 mm is sufficiently narrow to simulate a sharp crack for Iidate granite. The CT specimens were loaded to total failure using a screw driven testing machine. In order to calculate the J-integral value by Equation (3), different initial crack lengths were machined into each set of the specimen size.

Typical sets of load-load line displacement (P-δ_L) curve for Rock A are shown in Figure 4. Figures 4(a) and (b) indicate the P-δ_L curves obtained from the CT specimens with different initial crack lengths ($a_0/W = 0.5$ and 0.6) for specimen size 6 T and 2.5 T, respectively. It is noted in the 6 T size specimen (Fig. 4(a)) that the P-δ_L curve for the longer crack length specimen ($a_0/W = 0.6$) joins with that for the shorter crack length specimen ($a_0/W = 0.5$) at the displacement about 300 μm, demonstrating that the fracture process zone is fully formed in this specimen size. From the viewpoint of the deformation behavior, the test results of 6 T size specimen can be taken as valid for measuring the tension-softening curve of Rock A. On the other hand, the test records of 1.5 T, 2.5 T and 4 T size specimens indicate that the

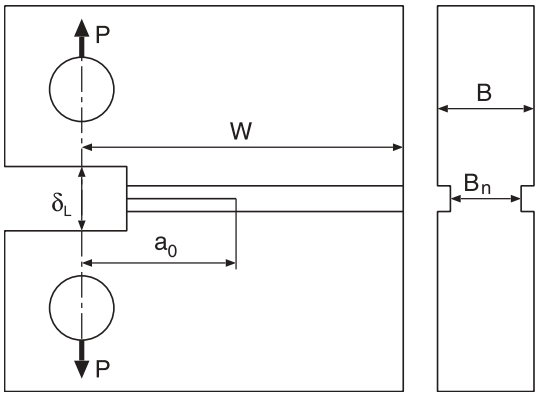

Figure 3
Geometry of the compact tension specimen used.

Table 2

Dimensions of the compact tension specimens used.

Rock	Nominal specimen size	a_0 (mm)	W (mm)	B (mm)	B_n (mm)
	1.5T (8)*	36–46	75	40	25
	2.5T (7)	50–74	125	50	33
	4Ta (2)	110, 133	222	60	40
A	6T (2)	150, 180	300	60	50
	1T** (1)	16.5	49.7	20.4	—
	3T** (1)	47.4	151	47.4	—
	4Tb** (1)	114	210	47.0	—
D	4T (2)	81, 90	180	60	41
F	2T (3)	45, 50	100	40	32
H	4T (2)	100, 120	200	61	47

*: Number of specimens used.
**: Crack growth resistance curve was measured.
Side grooves were not introduced.

specimen sizes are insufficiently large to allow the fracture process zone to extend entirely during the tests.

Following the procedure of the J-based technique, the tension-softening curves were deduced for each of specimen pairs from the experimentally obtained records of P-δ_L and δ_t-δ_L. For the 2.5 T size specimen of Rock A, several pairs of the specimens were tested to examine the reproducibility for the obtained result, after which the tension-softening curve was obtained for each pair of the specimens. Figure 5(a) gives the experimental scatter band for the tension-softening curve determined for the 2.5 T size specimen. An upper and lower bound are drawn to indicate the scatter of the resulting tension-softening curves. An averaged tension-softening curve shown in Figure 5(a) was determined by means of the least-square method from the tension-softening curves obtained. The averaged tension-softening curve is compared with the tension-softening curves obtained for 1.5 T, 4 T and 6 T size specimens.

Deduced tension-softening curves of Rock A for four specimen sizes by means of the J-based technique are indicated in Figure 5(b). The tension-softening curves shown in Figure 5(b) is the averaged data for each specimen size. Taking into account the scatter band of the tension-softening curve as observed for the 2.5 T size specimen, it can be seen that the tension-softening curves obtained for the specimen sizes greater than the 2.5 T size are approximately consistent with each other. However, the tension-softening curve of the 1.5 T size specimen slightly deviates from the general trend obtained for the larger specimens. This comparison demonstrates that the specimen size independent tension-softening curve can be determined by the J-based technique using subsized specimens.

The measured fracture parameters obtained by the J-based technique are summarized in Table 1 for Rock's A, D, F and H. Averaged values are given in Table 1. E' is the effective Young's modulus measured from the initial tangent of the

load-load line displacement curve of the fracture toughness specimens tested using the J-based technique (HASHIDA and TAKAHASHI, 1985). J_c is the critical J-integral value obtained from the area under the tension-softening curve. K_c is the critical stress intensity factor converted from the J_c value using the equation $K_c = \sqrt{E'J_c}$. σ_f is the peak value of the deduced tension-softening curve which corresponds to the uniaxial tensile strength by the definition of the tension-softening model. σ_{uts} is the tensile strength measured by a direct tensile test of Rock A and D (HASHIDA, 1990) in which only peak load was recorded. It can be seen that the σ_f value compares well with the σ_{uts} value for the two kinds of granites. This result supports the use of the J-based technique, which is an indirect method to measure the tension-softening curve of rock.

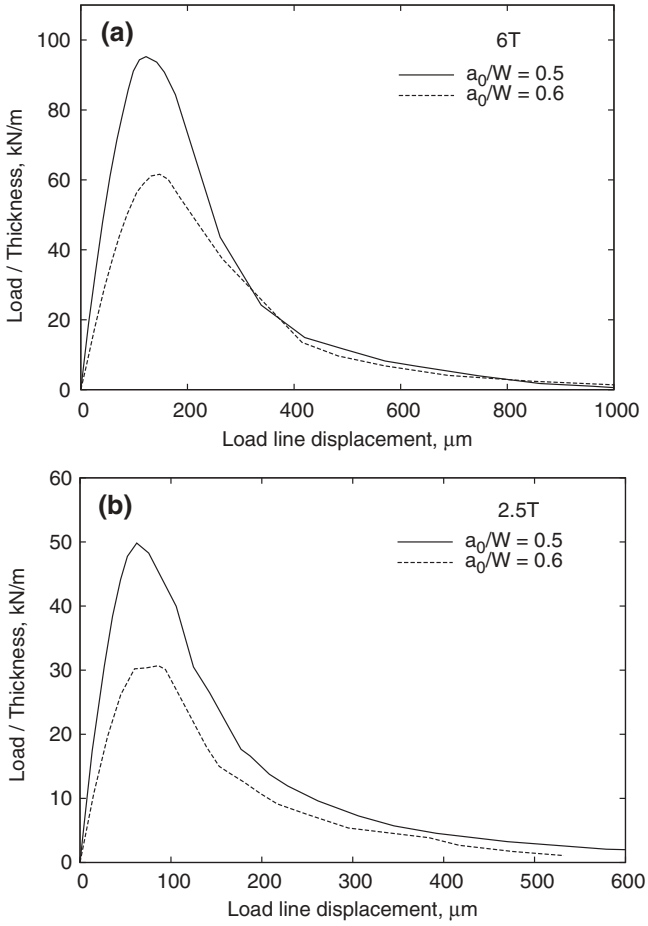

Figure 4
Load-load line displacement curves measured for two specimens with slightly different crack length. (a) is measured curves for 6 T size specimens and (b) is for 2.5 T size specimens.

Next, we examine the size dependency of the J-based technique from the viewpoint of fracture toughness. Figure 6 shows the critical J-integral values J_c determined for four specimen sizes of Rock A, which are computed from the deduced tension-softening curves. The J_c is plotted against the ligament size $W - a_0$ as the representative specimen size, where as the ligament size is the averaged value of the specimens used for the J-based tests. The fracture energy G_F (RILEM50-FMC, 1987) is also shown for comparison. The fracture energy G_F is calculated from the load-load line displacement record using the following equation

$$G_F = \frac{A}{B(W - a_0)}, \tag{4}$$

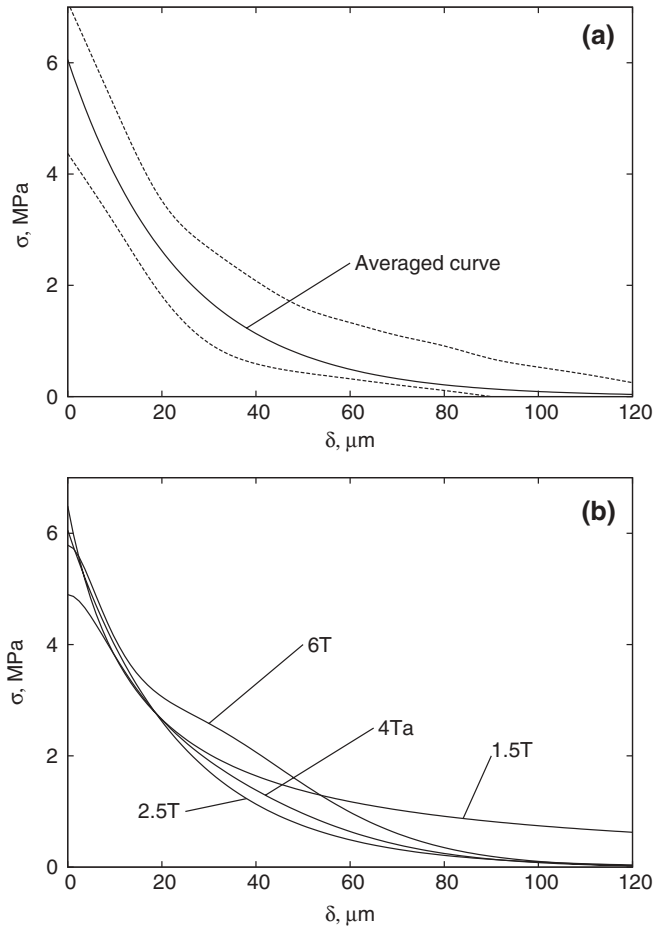

Figure 5
Tension-softening curves Deduced by the J-based technique. (a) deduced tension-softening curve for 2.5 T size specimen. Dashed line indicates the scatter band of the test results. (b) Summary of the deduced tension-softening curves for four specimen sizes.

where A is the area under the load-load line displacement curve, and B, W and a_0 are the specimen dimensions as shown in Figure 3, respectively. Since the side grove was introduced into the specimen used, B_n was used for B in Equation (4). The G_F values increase with the increase of the specimen size, and then tend to approach a constant value. It also has been shown that the critical stress intensity factor computed from the peak load of the fracture toughness specimens exhibits a significant specimen size dependency and no constant value is obtained with the specimen dimensions used (HASHIDA, 1990). In contrast, the J_c determined from the tension-softening relation provides a reasonably constant value irrespective of the different specimen sizes used. It is also noted that the J_c value is relatively close to the constant G_F value for the larger specimen sizes. The agreement of the two fracture parameters for the larger specimen sizes also supports the usefulness of the J_C, which may be applicable for the analysis of large-scale crack growth behavior in rocks. In the J-based technique, two specimens with slightly different crack lengths are used to evaluate the J-integral as a function of the deformation, whereas the G_F value is evaluated from the load-load line displacement data of one specimen. Even though the reason for the specimen size effects is still unclear, the above comparison may suggest that the differentiation method used in the J-based technique is more accurate for the determination of the true facture energy, compared with the G_F approach. However, a more detailed examination is needed to clarify the reason for the results shown in Figure 6. It might be considered that using two specimens in the J-based technique cancels out a size-dependent effect in rock specimens. The above-mentioned result indicates that the size-independent fracture toughness can be obtained using subsized specimens on the basis of the tension-softening model.

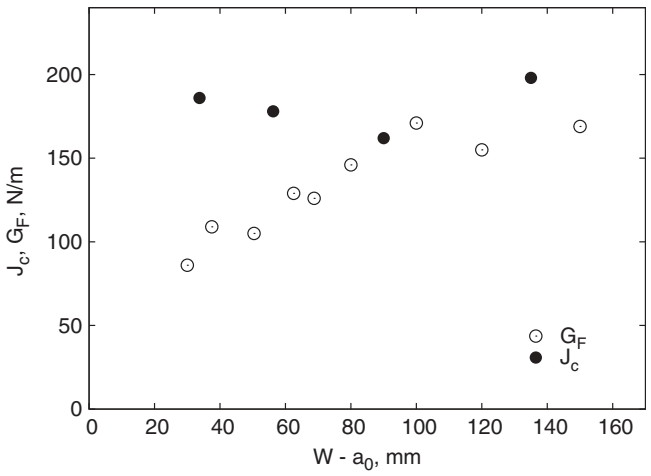

Figure 6
Comparison of the fracture energy G_F and the critical J-integral value J_c based on the tension-softening model.

Furthermore, we compare the fracture toughness K_c determined based on the tension-softening model with K-resistance curves. During the fracture toughness tests using CT specimens of Rock A, unloading and reloading cycles were frequently performed. Based on the unloading compliance data, the amount of crack growth Δa was determined (ISRM, 1988). The crack growth resistance is measured by the stress intensity factor for the unloading point. The measured K-resistance curves are summarized in Figure 7 for various CT specimens of Rock A. The K_c value computed from the J_c (see Table 1) is also indicated in Figure 7 for Rock A. The shaded region in Figure 7 shows the error band of the K_c values obtained from the determined tension-softening curves. The measured K-resistance is shown to initially increase, and then tends to saturate at the longer crack growth stage. In some test results (1 T, 1.5 T, and 6 T size specimens), the K-resistance shows a decreasing trend when the extending crack tip approaches the back surface of the specimen, probably due to the specimen end effect. Nonetheless, the general trend observed in Figure 7 suggests that the saturated K-resistance may be approximately in the range of 2.2–2.5 $MPam^{1/2}$. The range of K-resistance value is relatively close to the K_c value computed from the J_c. In order to predict the process of the crack growth in large-scale rock masses, it is necessary to evaluate the upper bound of the crack growth resistance corresponding to the steady-state crack growth condition. The above-mentioned result demonstrates that the crack growth resistance under the steady-state crack growth condition can be evaluated from the tension-softening relation using subsized specimens.

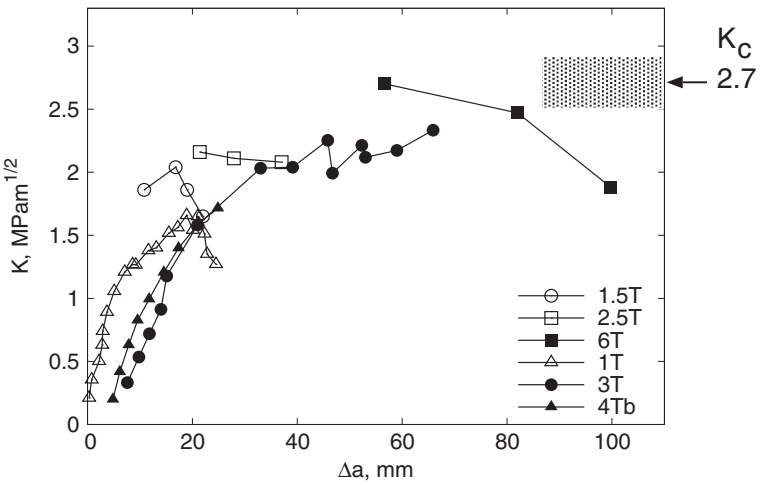

Figure 7
K-resistance curve of Rock A. K_c is the critical stress intensity factor calculated from the tension-softening curve. The shaded region indicates the scatter band of the K_c values.

This section discussed the validity of the fracture toughness evaluated on the basis of the tension-softening model. The next section describes the applicability of the tension-softening model to the analysis of the crack growth in hydraulic fracturing.

3. Hydraulic Fracturing

In this section, the results of hydraulic fracturing experiments are analyzed to deduce the crack growth resistance curve for Iidate granite, and then compared with the fracture toughness, by evaluation based on the tension-softening model. The loading configuration and crack geometry in the hydraulic fracturing experiment are quite different from those for the fracture toughness testing of compact tension specimens. Thus, the comparison may be useful to verify the validity of the fracture toughness evaluated based on the tension-softening model.

HASHIDA *et al.,* (1993) conducted a series of laboratory scale hydraulic fracturing tests using several rectangular specimens prepared from Rock F, as shown in Figure 8. As shown in Table 3, the sizes of the rectangular specimens were in the range of 15 cm-1m. The dimensions of the specimens are nominally designated by 15 cm, 20 cm, 30 cm, 50 cm, and 1 m. A simulated vertical borehole of 15 mm in diameter was drilled in the center of all specimens, and a bilobed pre-notch was introduced on the borehole using a specially designed devise in order to facilitate the analysis of crack propagation resistance. The depth of the pre-notches a_i/λ was approximately 0.5. In addition, larger-scale hydraulic fracturing tests have also been performed using a 10 m sized specimen, which was quarried at the quarry in Iidate as illustrated in Figure 9. The rock type used for the 10m sized specimen is designated as Rock H. Vertical boreholes, 48 mm in diameter were drilled into the 10 m sized specimen.

The hydraulic fracturing experiments were performed by pressurizing the borehole using rubber packers. A set of rubber packers with different pressurization intervals was utilized to extend the crack step by step in such a way that the subsequent injection interval enclosed the crack region created at the preceding stage. Dyed fluid was used as the pressurization fluid to delineate the hydraulically induced crack. After the tests, the specimen was broken open along the dyed crack plane to examine the crack growth process. In the following, we briefly describe a method for determining the crack propagation resistance, based on the results of the hydraulic fracturing tests. Schematics of crack propagation process and corresponding borehole pressure vs. crack length (P-Δa) are shown in Figure 10. We consider the pressure variation with crack growth during the stepwise pressurization. The locations A and B represent the positions of the rubber packer used for the hydraulic fracturing test. The pressurization interval for the first cycle is A-A, and B-B for the subsequent cycle, respectively. The point 1 on the P-Δa curve denotes the crack initiation from the pre-notch tip. When the crack tip along the borehole reaches the location A, the pressure decreases due to the leakage of the injection fluid without

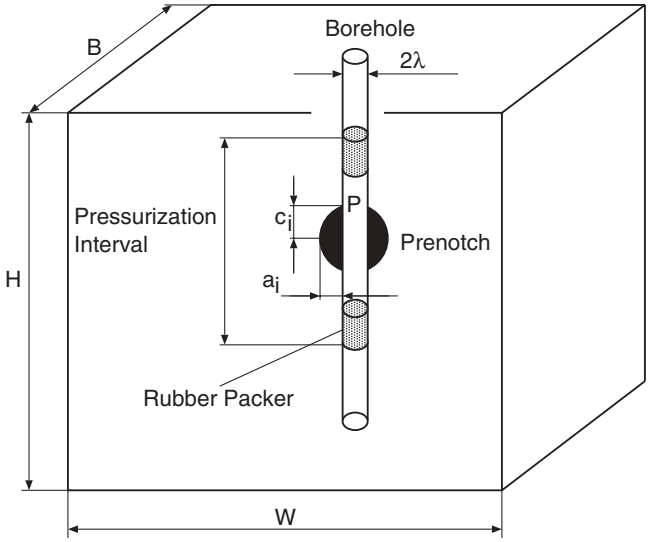

Figure 8
Specimen geometry used for laboratory scale hydraulic fracturing tests.

significant crack growth. At the subsequent cycle, where the borehole interval B-B is subjected to fluid injection, the crack starts to propagate after the pressure corresponding to the point 2 is reached. When the fluid gets over the straddle packer at the location B, the pressure decreases again. Thus, the borehole pressure, which corresponds to the crack length induced at the pressure $P(\Delta a)$ can be found by comparing the magnitude of the maximum pressure achieved at the cycle P_{pre} and that at the subsequent cycle P_{sub}. Namely, $P(\Delta a) = P_{pre}$, if $P_{pre} \leq P_{sub}$, and $P(\Delta a) = P_{sub}$, if $P_{pre} > P_{sub}$. This discussion enables us to determine the crack dimension corresponding to the borehole pressure, and then to construct crack propagation resistance curves obtained from hydraulic fracturing tests. For the 10 m sized specimen, in addition to the above-mentioned simple procedure, a detailed analytical investigation (Abé *et al.,* 1989) has been undertaken, in which the crack

Table 3

Specimen dimensions used for small-scale hydraulic fracturing tests.

Nominal specimen size	W (cm)	B (cm)	H (cm)	Borehole diameter 2λ (mm)
15 cm	15	15	15	15
20 cm	20	20	20	15
30 cm	30	30	30	15
50 cm	50	50	50	15
1 m	100	100	100	15

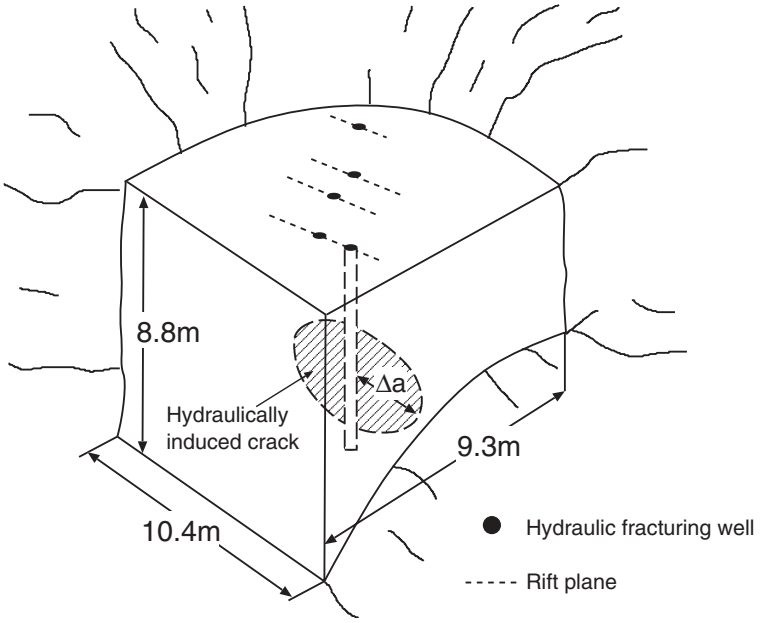

Figure 9
Geometry of the 10 m sized rock specimen for hydraulic fracturing test.

growth resistance data were obtained assuming that the stress intensity factor is uniform along the periphery of the hydraulically induced crack. In the analysis, the process of crack growth observed on the dyed fracture surface and borehole pressure vs. time records were used to evaluate the crack growth resistance as a function of the

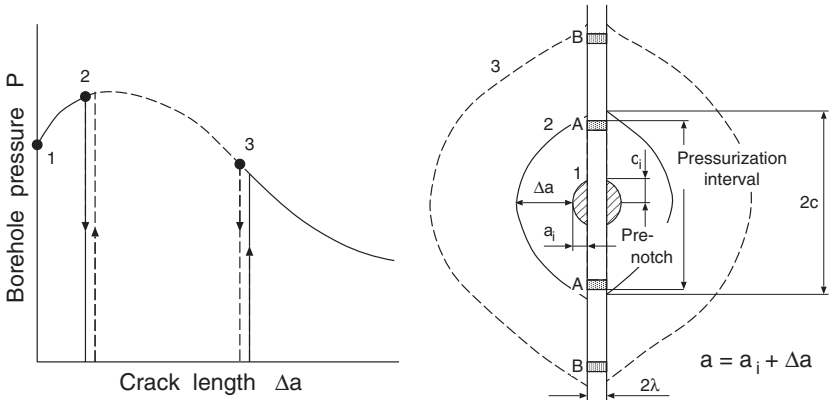

Figure 10
Procedure for the analysis of crack growth resistance in hydraulic fracturing test.

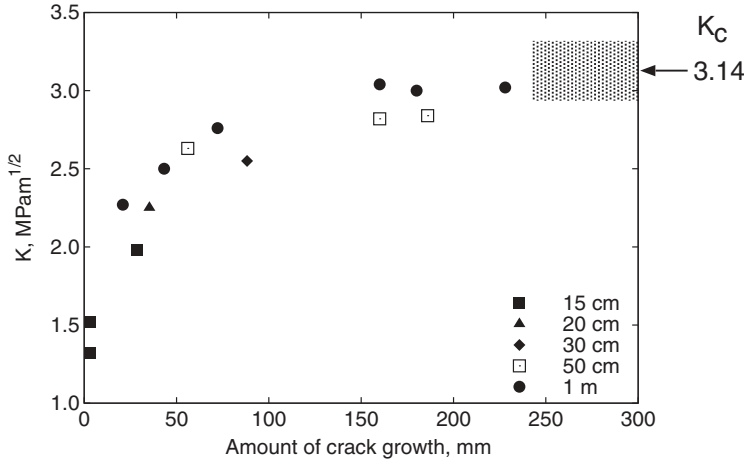

Figure 11
Crack growth resistance curve measured by hydraulic fracturing tests. K_c is the critical stress intensity factor calculated from the tension-softening curve. The shaded region indicates the scatter band of the K_c values.

crack length. For detailed information of the experimental procedures used for the hydraulic fracturing experiments and the analytical methods, the reader is referred to the literature (HASHIDA *et al.,* 1993: ABÉ et al. 1989).

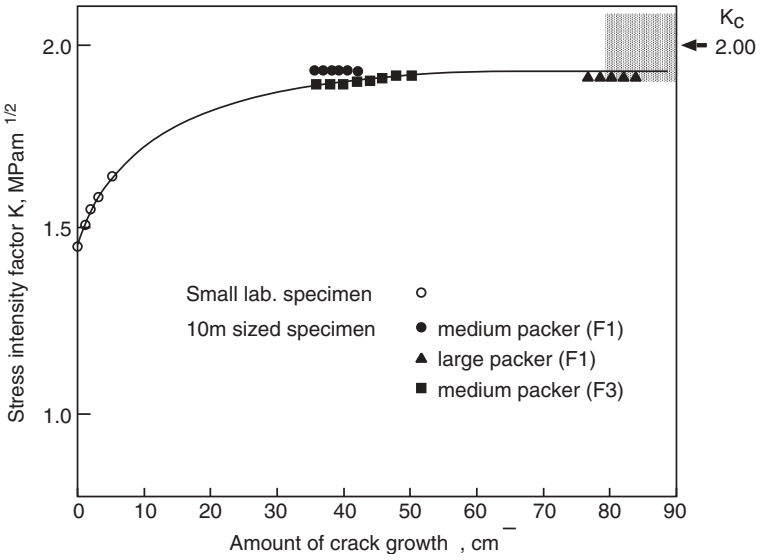

Figure 12
Crack growth resistance curve measured by the 10 m sized rock specimen. K_c is the critical stress intensity factor calculated from the tension-softening curve. The shaded region indicates the scatter band of the K_c values.

The crack propagation resistance curves determined are summarized for the hydraulic fracturing tests conducted on Rock F and H in Figures 11 and 12, respectively. Figure 12 gives the experimental data from the hydraulic fracturing tests conducted on the two boreholes (F1 and F3) that were drilled into the 10 m sized specimen. It has been shown that the aspect ratio of the induced cracks a/c was in proximity to 1.0, particularly for the longer crack growth stage, indicating that the induced cracks in the hydraulic fracturing experiments were approximately of circular shape. It is seen that the crack propagation resistance initially increases and gradually levels off as the crack extension progresses. It is particularly noted that the curve effects a nearly constant crack propagation resistance, and a steady-state crack growth condition is achieved at the larger crack growth stage. The so-called rising R-curve behavior observed in Figures 11 and 12 is consistent with the growth of fracture process zone. The fracture toughness value determined by the J-based testing method K_c is also indicated in those figures. Note that the constant crack propagation resistance at the larger crack growth stage is close to the K_c. In order to assess the crack growth process in large-scale rock masses, it is necessary to evaluate an upper limit of fracture toughness values. These results suggest that the K_c determined by the J-based method is judged to be an appropriate fracture toughness value which may be applicable to the analysis of crack growth in hydraulic fracturing.

4. Concluding Remarks

This paper discusses the usefulness of the tension-softening model in the determination of the appropriate fracture toughness of rocks. The validity of the tension-softening model was discussed by comparing the experimental results of fracture toughness tests and laboratory scale hydraulic fracturing tests conducted on Iidate granite. The fracture toughness test results demonstrated that the evaluation method based on the tension-softening model allowed us to measure the specimen size-independent fracture toughness of the rock using subsized specimens. It was also established from the fracture toughness test results that the size-independent fracture toughness corresponded to the constant value of the crack growth resistance in the steady-state condition. The fracture toughness evaluated using the tension-softening model was compared with the crack propagation resistance obtained from the hydraulic fracturing tests. The results suggested that the tension-softening model may be able to provide an appropriate fracture toughness for predicting the large-scale crack growth induced by hydraulic fracturing.

References

Abé, H., Hayashi, K., and Hashida, T. *Studies on crack propagation resistance of rocks based on hydrofrac data of large specimens*. In Proc. SEM-RILEM *Int. Conf. on Fracture of Concrete and Rock* (S. P. Shah and S. E. Swartz eds.) (Houston 1989), pp. 354–361.

HASHIDA, T. *Tension-softening curve measurements for fracture toughness determination in granite*. In *Fracture Toughness and Fracture Energy* (Mihashi, H., Takahashi, H., and Wittmann, F. H. eds.) (A. A. Balkema 1989) pp. 47–55.

HASHIDA, T. (1990) *Evaluation of fracture processes in granites based on the tension-softening model*. In *Micromechanics of Failure of Quasi-Brittle Materials* (Mihashi, H., Takahashi, H., and Wittmann, F. H. eds.) (Elsevier Applied Science, 1990) pp. 233–243.

HASHIDA, T, SATO, K., and TAKAHASHI, H. (1993), *Significance of crack opening monitoring for determining the growth behavior of hydrofractures*. In Proc. 18th *Workshop on Geothermal Reservoir Eng*. (Stanford University, Stanford, 1993) pp. 241–246.

HASHIDA, T. and TAKAHASHI, H. (1985), *Simple determination of the effective Young's modulus of rock by the compliance method*, J. Test. Evaluat. *13,* 77–84.

HASHIDA, T. and TAKAHASHI, H. (1993), *Significance of AE Crack Monitoring in Fracture Toughness Evaluation and Non-linear Rock Fracture Mechanics*, Int. J. Rock Mech. Min. Sci. and Geomech. Abstr. *30*–1, 47–60.

HILLERBORG A. *Analysis of one single crack*, In *Fracture Mechanics of Concrete* (F. H. Wittmann ed.) (Elsevier Science Publishers B. V., Amsterdam 1983) pp. 223–250.

INGRAFFEA, A. R. *Theory of crack initiation and propagation in rock*. *In Fracture Mechanics of Rock* (Atkinson, B. K. eds.) (Academic Press 1987) pp. 71–110.

ISRM COMMISSION ON TESTING METHOD (1988), *Suggested method for determining fracture toughness of rock*, Int. J. Rock Mech. Min. Sci.and Geomech. Abstr. *25*–1, 71–96.

LABUZ, J. F., SHAH, S. P., and DOWDING C. H. (1987), *The fracture process zone in granite: Evidence and effect*, Int. J. Rock. Mech. Min. Sci. and Geomech. Abstr. *24*–4, 235–246.

LI, V. C., CHAN, C. M., and LEUNG, C. K. Y. (1987), *Experimental determination of the tension-softening relations for cementitious composites*, Cem. and Conc. Res. *17*, 441–452.

RILEM50-FMC (1987) *Determination of the fracture energy of mortar and concrete by means of three-point bend tests on notched beams*, Mate. Struct. *18*–106, 45–48.

SCHMIDT, R. A. and LUTZ, T. J. (1979), *K_{Ic} and J_{Ic} of Westerly granite — effects of thickness and in-plane dimensions*. In *Fracture Mechanics Applied to Brittle Materials* (Freiman, S. W. ed.) (ASTM STP 678, 1979) pp. 166–182.

(Received February 28, 2005, Revised/accepted November 4, 2005)